Applied Geochemistry 167 (2024) 106003

Contents lists available at ScienceDirect

Applied Geochemistry

journal homepage: www.elsevier.com/locate/apgeochem

Cation exchange parameters for Opalinus Clay and its confining units

Paul Wersin *, Lukas Aschwanden, Mirjam Kiczka

Rock-Water Interaction, Institute of Geological Sciences, University of Bern, Baltzerstrasse 1+3, 3012, Bern, Switzerland

A R T I C L E I N F O

Editorial Handling by: Dmitrii A. Kulik

Keywords:
Cation exchange
Selectivity coefficients
Opalinus Clay
Confining units

A B S T R A C T

The knowledge of cation exchange parameters is important to understand and model the porewater chemistry in clayrocks. The Opalinus Clay (OPA) is a well-studied formation in view of its importance as host rock for radioactive waste repositories, but uncertainties exist regarding its cation exchange parameters, in particular its selectivity coefficients (K_c). In fact, porewater chemistry models for OPA have so far been based on generic selectivity coefficients.

Thanks to a recent extensive siting programme, involving eight vertical deep boreholes in northern Switzerland, a large number of porewater and cation exchange data from the OPA and its clay-rich confining units could be analysed. Thus, from the combination of porewater compositions (obtained from high-pressure squeezing and advective displacement), and exchangeable cation data (obtained from Ni ethylenediamine extraction), reliable selectivity coefficients could be derived. The values for $K_c^{Na/K}$, $K_c^{Na/Ca}$, $K_c^{Na/Mg}$ are consistent with those obtained in parallel from the Mont Terri underground rock laboratory although the scatter is somewhat larger in the latter dataset. The derived selectivity coefficients indicate no dependency on ionic strength or *in-situ* temperature. Minor differences in K_c values between OPA and confining units can be attributed to differences in clay mineralogy. The validity of a two-site cation exchange model including illite and smectite for estimating exchangeable Na, Ca and Mg from measured porewater compositions could be shown, while this simple model underpredicts the share of exchangeable K. The exchangeable cation extraction procedure induces the dissolution of Sr-bearing minerals whose amount is in the same range as exchangeable Sr, thus not enabling the derivation of selectivity coefficients for Sr.

Finally, derived selectivity coefficients confirm results of previous studies, thus providing confidence in the applied experimental and modelling protocols on the one hand and in the outcome of those studies on the other hand.

1. Introduction

Low permeability argillaceous rocks (clayrocks) have been gaining increasing interest in view of their sealing and barrier properties for engineering applications, such as for gas storage, geothermal energy or waste disposal (Charlet et al., 2017). Clayrocks with sufficient thickness are foreseen as host rocks of geological repositories for radioactive waste, such as the Boom Clay in Belgium (Ondraf/Niras 2001), the Callovo-Oxfordian (COx) Formation in France (Andra 2005) or the Opalinus Clay (OPA) in Switzerland (Nagra 2002, 2014). Besides their sealing properties, these rocks act as efficient sorbent for radionuclides and as buffer against chemical disturbances (Beaucaire et al., 2004; Wersin et al., 2020). Regarding the latter function, the high cation exchange capacity (CEC) of clayrocks helps to buffer the cation concentrations and their shares in the porewater via cation exchange reactions (Tournassat et al., 2015).

Cation exchange is also an important component in modelling of porewater chemistry for these rock types (Gaucher et al., 2009; Pearson et al., 2011; Frederickx et al., 2018). In this context, it is important to rely on robust cation exchange parameters, such as exchange coefficients. These may vary as a function of many variables, such as the porewater composition, its ionic strength and pH and the nature of the clay mineral assemblage (McBride 1994; Thellier and Sposito 1989; Tournassat et al., 2009). Regarding the COx and the OPA, different types of cation exchange models have been discussed in literature including single-site and multi-site models based on the Vanselow or Gaines-Thomas convention or including surface activity species (Pearson et al., 2003; Tournassat et al., 2007, 2009). For modelling the porewater chemistry of these clayrocks, it has been shown that a single site model based on the Gaines-Thomas convention is appropriate (as

* Corresponding author.
E-mail address: paul.wersin@unibe.ch (P. Wersin).

https://doi.org/10.1016/j.apgeochem.2024.106003
Received 9 January 2024; Received in revised form 28 March 2024; Accepted 6 April 2024
Available online 7 April 2024

long as the cation compositions do not show strong variations across the formation) (Tournassat et al., 2007, 2009; Gaucher et al., 2009). In this convention, an exchange reaction can be described as:

$$z_B AX + z_A B \leftrightarrow z_A BX + z_B A \quad (1)$$

where A and B are cations in solution with their charges z_A and z_B and AX and BX are the corresponding (exchangeable) cations on the exchanger X.

Under given experimental conditions one can define a conditional equilibrium constant, usually termed selectivity coefficient, for the exchange of A by B:

$$K_c^{A/B} = N_B^{z_a}/N_A^{z_b} \text{ x } a_A^{z_b}/a_B^{z_a} \quad (2)$$

where N_A and N_B are the charge (or equivalent) fractions on the exchanger and a_A and a_B are the activities in solution of cations A and B.

The OPA has been extensively studied in terms of its mineralogical, geochemical, mechanical and hydraulic characteristics over the last 25 years (Bossart et al., 2017; Mazurek et al., 2023) and can thus be considered as important reference material for clayrocks serving as seals or barriers. Regarding cation exchange, a large body of data exists from the Mont Terri rock laboratory and deep boreholes in Switzerland (Pearson et al., 2003; Wersin et al., 2020, Marques Fernandes et al., 2024). Robust data regarding selectivity coefficients for cation exchange are however lacking. Early attempts were made within the Mont Terri Project using different cation extraction methods but in view of scatter in data no selectivity coefficients were recommended (Pearson et al., 2003). Based on Nickel ethylenediamine (Ni-en) extraction data of one sample, Bradbury and Baeyens (1998) proposed values for Na–K, Na–Ca, and Na–Mg selectivity coefficients. Later, Pearson et al. (2011) and Wersin et al. (2016) applied selectivity coefficients based on values derived for the COx (Gaucher et al., 2009) in view of lack of reliable data available for OPA.

Recently, an extensive drilling campaign (termed TBO) has been carried out in northern Switzerland with the aim to explore the OPA with regard to its suitability as host rock for radioactive waste disposal in three siting regions (Mazurek et al., 2023). Within the scientific TBO programme, a large number of drillcore samples from OPA and its overlying and underlying low permeability units (so-called confining units) were analysed for porewater chemistry and cation exchange characteristics. A large dataset on CEC and exchanger composition could be obtained using Ni-en and Cs extraction methods (Baeyens and Marques Fernandes 2022, Marques Fernandes et al., 2024). In parallel, porewaters were extracted from drillcores by the squeezing and advective displacement methods leading to a comprehensive dataset on porewater chemistry (Kiczka et al., 2023).

The intention of this study is to improve the knowledge on cation exchange parameters and to provide a robust database of selectivity coefficients for an otherwise well-characterised argillaceous rock sequence. To this end, the cation exchange and porewater data for OPA and its confining units generated within the TBO programme (TBO samples) are analysed. The analysis is complemented with corresponding data on OPA from the Mont Terri rock laboratory (Mont Terri samples) acquired over the last 25 years (Wersin et al., 2022a). Regarding cation exchange, the focus is on Ni-en extraction data which are deemed more appropriate for deriving selectivity coefficients compared to Cs extraction. The latter extraction method leads to an enhanced mobilisation of potassium presumably from illitic particles due to the strong selectivity of Cs for frayed edge sites of illite (Marques Fernandes et al., 2024). The main goal is to derive selectivity coefficients of major cations (Na, Ca, Mg, K) for OPA and its confining units based on TBO and Mont Terri samples and to compare these with previous datasets of OPA and other clayrock formations. For this purpose, the data on CEC and exchanger compositions are first summarised before selectivity coefficients are derived. A further goal is to evaluate effects of ionic strength and *in-situ* temperature. Finally, selectivity coefficients to be used for porewater modelling are recommended.

2. Materials and methods

2.1. Background information and sample origin

The Opalinus Clay (OPA) is a Mesozoic (Dogger) clay-rich rock that extends across a large area in northern Switzerland. It is vertically and laterally homogeneous with a thickness of about 100 m, consisting predominantly of clay minerals (~35–75 wt.-%), quartz (~10–30 wt.-%), calcite (~10–30 wt.-%) and feldspar (~1–5 wt.-%) (Wersin et al., 2020; Mazurek et al., 2023). The clay minerals in the fraction <2 μm consist mainly of illite, illite/smectite mixed layers and kaolinite, whereas chlorite contents are subordinate. The overlying unit, termed Dogger above Opalinus Clay (D.A.O) is much more heterogeneous, both vertically and horizontally with thicknesses of 80–150 m and consists of clay-rich lithologies alternating with more calcareous ones. The underlying rather thin (~50 m) Liassic unit (Staffelegg Fm.), termed Lias here, is generally clay-rich but vertically heterogenous and contains lithologies dominated by marls, sandstones or limestone. Due to their generally low-permeability character, the overlying and underlying units D.A.O. and Lias, respectively, are often called confining units. The clay minerals in these units also mainly consist of illite, illite/smectite mixed layers and kaolinite, but the share of kaolinite is more variable and generally smaller than in OPA (Mazurek et al., 2023).

The samples collected from the TBO programme (TBO samples) include drillcores from the Opalinus Clay as well as from the confining units. These stem from eight deep boreholes (BOZ1-1, BOZ2-1, BAC1-1, STA2-1, STA3-1, BUL1-1, MAR1-1, TRU1-1) located in three study areas (Jura Ost – JO, Nördlich Lägern – NL and Zürich Nordost – ZNO) within an area of ~50 × 10 km^2 at the northern border of the Swiss Molasse basin (Fig. 1). The Opalinus Clay in this region occurs at depths of 530–950 m below surface (referring to the centre of the formation). *In-situ* temperatures depend on depth, ranging from ~30 to ~50 °C in the OPA.

The Mont Terri rock laboratory is located in NW Switzerland in the Jura mountains (Fig. 1). It transects the Opalinus Clay which lies within an asymmetric anticline structure in the Jura fold-and-thrust belt about 300 m below surface (Bossart 2007). The strata dip at angles ranging from 22° in the north to 55° in the south. *In-situ* temperatures are around 13 °C.

2.2. Cation exchange experiments

The Ni-en extraction method (Baeyens and Bradbury, 1994; Bradbury and Baeyens 1998) is based on the strong adsorption of the Ni-en complex and the release of the exchangeable cations into solution. This method has been improved for clayrock samples (Hadi et al., 2019) leading to a refined experimental protocol (RWI 2020). An important aspect is the high solid/liquid ratio which minimises carbonate mineral dissolution during the extraction. The cation exchange capacity (CEC) can be determined by two ways: (i) by the difference in Ni concentrations in the original stock solution compared to the extract solution and (ii) by the sum of released cations minus the sum of released anions. In addition, the exchanger composition and the fractional occupancies of the cations can be derived. For the latter, the proportion of the cations needs to be corrected for the contribution of dissolved salts and mineral dissolution as outlined in Section 2.5.

Extraction of samples from the drillcores of the deep TBO boreholes, their on-site conditioning and storage before the experiments, was carried out by a standardised protocol (Rufer and Stockhecke 2021) with the aim to minimise evaporation, oxidation and outgassing. Samples were prepared for Ni-en extraction by removing the core rim and disintegrating the central part of the drillcore sections to 0.5–1 cm sized fragments. Thirty grams of this water saturated material was added to 30 g of degassed Ni-en solution (leading to a solid/liquid ratio of ~0.9).

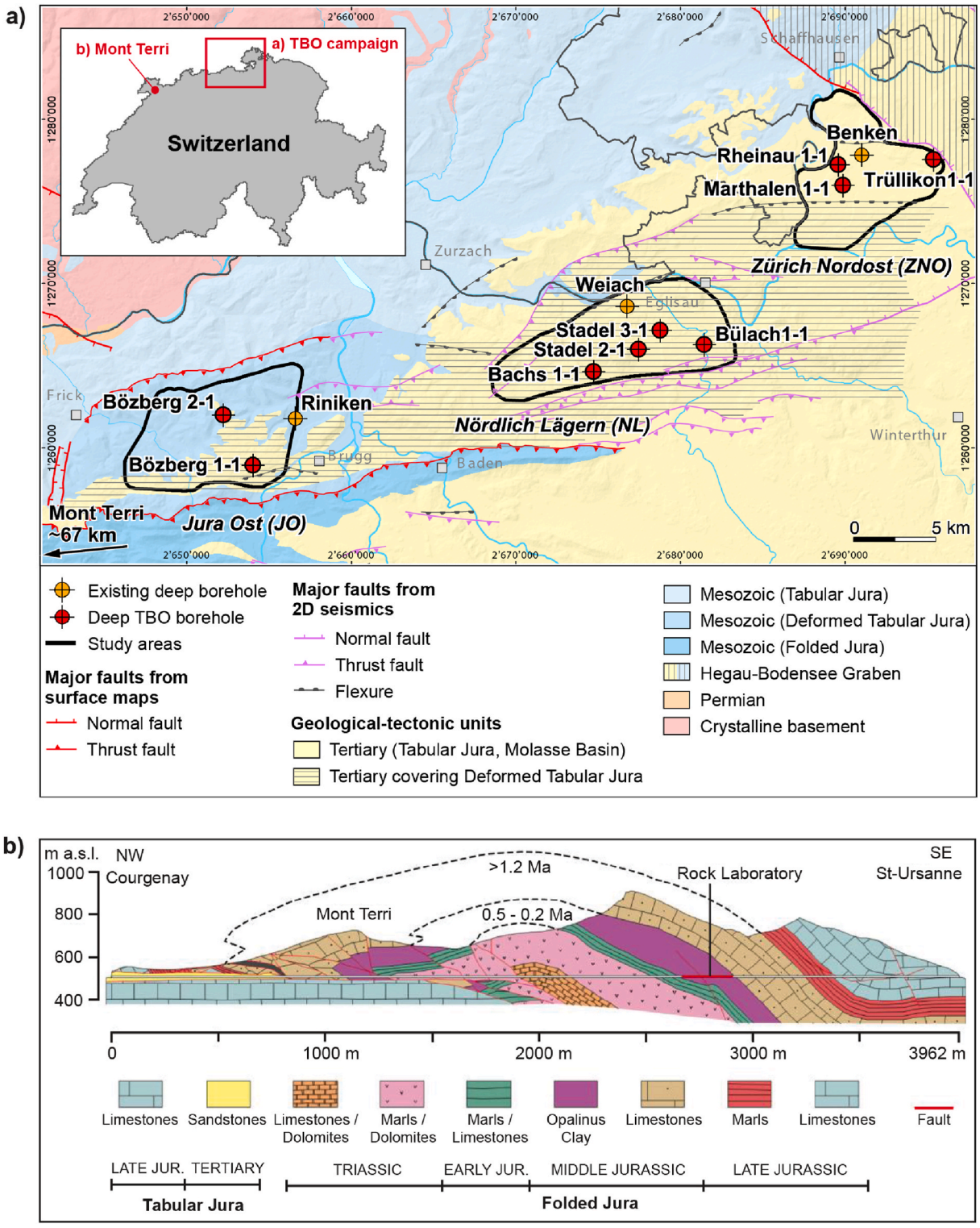

Fig. 1. a) Location of deep boreholes from TBO programme and geological-tectonic map in northern Switzerland; b) Cross-section through the Mont Terri rock laboratory located in NW Switzerland.

Suspensions were shaken end-over-end for 24 h in an anaerobic chamber (95:5 N_2:H_2 atmosphere equipped with two Pd catalysts), followed by centrifugation and filtration through 0.2 μm millipore filters. Analyses of cations (Na, Ca, Mg, K, Sr, Ni and optionally Ba and Fe) were conducted with inductively coupled plasma spectrometry (ICP-OES), whereas anions (Cl, SO_4, F) were analysed by ion chromatography (IC). The analytical errors are ±7% for Na and Ca, ±9 % for Mg, ±5% for K, ±4% for Sr and ±6% for Ni. Detailed methodological procedures are documented in RWI (2020).

In the case of the data from the Mont Terri rock laboratory, only core samples from OPA for which Ni-en extracts were performed at high solid/liquid ratios were used for determining the cation exchange parameters. The selection is based on the synthesis study of Wersin et al. (2022a) and includes investigations of Bradbury and Baeyens (1998), Waber et al. (2003), Koroleva et al. (2011) and Hadi et al. (2019). Additionally, four samples reported in Aschwanden et al. (2024) and Lehmann (2021) were included in the analysis. Note that for most of the Mont Terri samples no anion analyses of the Ni-en extracts were performed. The information on anions was then taken from the corresponding aqueous extracts, which were performed at a similar S/L ratio.

2.3. Extraction and analysis of porewaters

Porewater was extracted from drillcores of the TBO programme by the high-pressure squeezing (SQ) and advective displacement (AD) methods. Prior to extraction, the drillcore samples were conditioned on-site and stored in the same way as mentioned in the previous section. The SQ and AD methods are described in detail in Kiczka et al. (2023). In short: Squeezing of selected cores to extract porewater was performed at pressures of 200–500 MPa. Here, only the experiments at the lowest pressure, which are deemed to reflect *in-situ* conditions most closely (Mazurek et al., 2015; Kiczka et al., 2023), are used in the analysis. In the case of AD, a large hydraulic gradient was applied to a confined rock sample, by which porewater was displaced by artificial porewater injected from the bottom. The displaced porewater samples with volumes of a few hundreds of μL were collected. After discarding the first syringe the next two syringes were considered to best reflect *in-situ* porewaters and these data are reported here. Water collected from squeezing and advective displacement were analysed for pH, cations (Na, K, NH_4, Ca, Mg, Sr) and anions (F, Cl, Br, NO_3, SO_4) with IC. Analytical uncertainties were ±4 % for Mg and NH_4, ±5 % for Cl and F, ±6 % for SO_4, NO_3, ±8 % for Ca and ±10 % Sr.

Regarding Mont Terri porewaters, data from waters sampled in packed-off boreholes as selected by Wersin et al. (2022a) were considered. This included both seepage waters (porewaters entering the borehole via large hydraulic pressure) and diffusively equilibrated waters (artificial water exchanging solutes with formation water until attainment of diffusive equilibrium). Analytical errors for major solutes are reported to be ±5% but the overall uncertainty may be higher as indicated for example from comparison of analyses obtained by different laboratories (Pearson et al., 2003).

2.4. Mineralogy and water content

The preparation of samples from the conditioned drillcores (see above sections) involved the rapid removal of rims to obtain uncontaminated material from the central part of the core. Water content was obtained from drying of about 200 g rock chips of a few mm^3 at 105 °C until weight constancy. Bulk mineralogical composition was quantified by a combination of X-ray diffraction and chemical data (S, C_{inorg}, C_{org}). Clay mineralogy was obtained from X-ray patterns of the <2 μm fraction. Details pertinent to methods and procedures are provided in RWI (2020). The identification and the quantification of clay mineral phases was based on oriented powder X-ray diffraction patterns (dry, glycolated, heated). For the quantification of the relative proportions of clay minerals, a full pattern fit in-house method analogous to the ARQUANT approach (Blanc et al., 2007) was used. Absolute clay contents were calculated by difference (total minus sum of all non-clay minerals). The identified clay minerals the include illite, illite/smectite mixed layers, kaolinite, chlorite and chlorite/smectite mixed layers. These are expressed as endmembers of illite, smectite, kaolinite and chlorite in this study.

2.5. Data selection and treatment

Ni-en extraction data of TBO samples from the boreholes BOZ1-1, BOZ2-1, BUL1-1, BAC1-1, STA2-1, STA3-1, MAR1-1 and TRU1-1 have been reported in data reports (Wersin et al., 2022b; Gimmi et al., 2022; Mazurek et al., 2021; Gaucher et al., 2023; Aschwanden et al., 2021; 2023; Zwahlen et al., 2022 Mäder et al., 2021; Aschwanden et al., 2023). Cation exchange parameters (Ni consumption, sum of cations, amounts of extracted Na, Ca, Mg, K and Sr) are listed together with clay-mineral contents, contents of illite, smectite, kaolinite and chlorite, as well as the water content in Table A1, Supplementary Material (SM)). Regarding Mont Terri samples, the corresponding information is shown in Table A2 (SM). Note that for these samples no clay mineralogy data is available.

The CEC can also be estimated based on the amounts of present clay minerals (illite, smectite, chlorite, kaolinite) contributing to this parameter (Wersin et al., 2016, Marques Fernandes et al., 2024). For the calculation of this theoretical CEC (CEC_{calc}) the reported CEC values of pure minerals were considered: 225 meq/kg for illite (Baeyens and Bradbury, 1994), 869 meq/kg for smectite (Karnland et al., 2006), 50 meq/kg for chlorite and 30 meq/kg for kaolinite (Allard et al., 1983).

Porewater chemistry data from TBO samples (SQ and AD waters) selected for this study are listed in Table A3 (SM). The selected porewaters originated either from the same drillcore (many AD samples) or from drillcores located in the vicinity of the respective cation exchange sample (usually within 10 m distance, however in a few cases the closest porewater sample was located up to 40 m away). This resulted in a total of 60 cation exchange/porewater sample pairs, of which 27 were from the OPA, 18 from the D.A.O and 15 from the Lias. Regarding the 11 Mont Terri samples, the porewater composition (Na, Ca, Mg, K, Sr, Cl, SO_4) associated to the cation exchange sample was estimated from the well-established cationic and anionic profiles across the formation (Wersin et al., 2022a) as illustrated in Figure A1 (SM). The resulting porewater compositions are shown in Table A.4 (SM).

In order to derive the exchanger composition and the fractional occupancies of the exchangeable cations the Ni-en extraction data need to be corrected for the contribution of dissolved salts and the (potential) dissolution of minerals during the extraction process. The dissolution of carbonate minerals (calcite, dolomite) is minimised by the applied experimental procedure as indicated from the study of Hadi et al. (2019) and the very low TIC concentrations in the high S/L extracts. Two correction methods (Bradbury and Baeyens 1998) were applied by attributing the main dissolved anions (Cl^- and SO_4^{2-}) to the main dissolved cations (Na^+ and Ca^{2+}) in different ways. In method 1, exchangeable Na is derived by correcting total Na with extracted Cl and SO_4, whilst in method 2, both total Na and Ca are corrected by correcting with extracted Cl and SO_4, respectively. In addition, a third correction method in which the anionic load is distributed among all extracted cations was tested as discussed in section 3.5. After correction, the cation occupancies of Na, K, Ca and Mg (equivalent scale) were calculated by normalising to the dry weight of the rock samples:

$$N_M = [M]/\ \Sigma Cations \quad (3)$$

Where N_M and [M] are the occupancy (equivalent fraction) and concentration (meq/kg), respectively, of Na, K, Ca or Mg and ΣCations is the (corrected) sum of exchangeable cations (meq/kg). Note that Sr was not included to derive the fractional occupancies because of the issue of mineral dissolution as discussed in section 4.3. In any case, the amount of extracted Sr was much lower than those of the other cations.

Table 1
Mean selectivity coefficients and standard deviation for $K_c^{Na/K}$, $K_c^{Na/Ca}$ and $K_c^{Na/Mg}$. Selectivity coefficients for illite, montmorillonite and the Callovo-Oxfordian formation (COx) also shown.

	Data type	Number of samples	$K_c^{Na/M}$ Method 1	Std-dev ±1 σ	$K_c^{Na/M}$ Method 2	Std-dev ±1 σ	$K_c^{Na/M}$ Other data	Ref.
Na^+- > K^+	all TBO data	60	18.1	±7.0	16.5	±6.0		this work
	D.A.O.	18	20.1	±9.4	18.0	±7.6		"
	OPA (TBO)	27	16.0	±5.3	14.9	±4.9		"
	Lias	15	19.2	±5.7	17.5	±5.2		"
	OPA (MT)	11	18.5	±2.5	17.2	±2.5		"
	Illite						12.9	a
	Montmorillonite						4.0	b
	COx						17.0	c
Na^+- > Ca^{2+}	all TBO data	60	9.8	±4.2	7.3	±2.3		this work
	D.A.O.	18	11.8	±6.5	8.3	±2.9		"
	OPA (TBO)	27	8.5	±2.3	6.9	±1.9		"
	Lias	15	9.9	±2.6	6.5	±0.8		"
	OPA (MT)	11	8.6	±1.1	6.5	±2.5		"
	Illite						11.0	a
	Montmorillonite						2.6	b
	COx						4.7	c
Na^+- > Mg^{2+}	all TBO data	60	9.2	±4.3	7.6	±2.7		this work
	D.A.O.	18	10.6	±6.5	8.3	±3.5		"
	OPA (TBO)	27	7.9	±2.6	7.0	±2.3		"
	Lias	15	9.9	±2.8	8.1	±2.1		"
	OPA (MT)	11	6.2	±1.4	5.3	±1.2		"
	Illite						11.0	a
	Montmorillonite						2.2	b
	COx						6.0	c

[a] Bradbury and Baeyens (2009).
[b] Bradbury and Baeyens (2003).
[c] Gaucher et al. (2009).

Table 2
Comparison of selectivity coefficients (in log-units) for TBO data obtained from different correction methods accounting for the contribution of dissolved salts (see text).

		$logK_c$ Method 1 ($NaCl/Na_2SO_4$)	±1σ	$logK_c$ Method 2 ($NaCl/CaSO_4$)	±1σ	$logK_c$ Method 3 (distributed)	±1σ
$Na^+ \rightarrow K^+$	all TBO data	1.26	±0.17	1.22	±0.16	1.18	±0.16
	OPA	1.20	±0.15	1.17	±0.14	1.15	±0.14
	CUs	1.29	±0.18	1.25	±0.17	1.21	±0.17
Na + - > Ca^{2+}	all TBO data	0.99	±0.15	0.86	±0.13	0.89	±0.12
	OPA	0.93	±0.12	0.84	±0.12	0.86	±0.12
	CUs	1.04	±0.16	0.89	±0.13	0.91	±0.13
Na + - > Mg^{2+}	all TBO data	0.96	±0.16	0.88	±0.14	0.85	±0.13
	OPA	0.90	±0.13	0.84	±0.13	0.82	±0.13
	CUs	1.01	±0.17	0.91	±0.15	0.88	±0.13

In order to derive exchange selectivity coefficients the activities of the respective cations need to be known (see eq. (2)). The activities of Na^+, Ca^{2+}, Mg^{2+} and K^+ were calculated from the porewater compositions using the geochemical code PHREEQC (Parkhurst and Appelo 2013) and the thermodynamic database THERMOCHIMIE Version 11 (Giffaut et al., 2014; Rodriguez et al., 2022). For the TBO samples, a temperature of 25 °C was considered, which is close to the temperature of the porewater extraction tests (squeezing, advective displacement). On the other hand, a temperature of 13 °C was considered for the Mont Terri samples, which corresponds to the temperature of the borehole water samples used for the derivation of the selectivity coefficients.

Table 3
Recommended selectivity coefficients (log-scale) and comparison with previously used ones for Opalinus Clay.

	Recommended from this study	Used previously	COx[f]	Boom Clay[g]
$Na^+ \rightarrow K^+$	1.2[a]	1.2[c,d]/1.4[e]	1.2	1.5
Na + - > Ca^{2+}	0.8[a]	0.7[c,d,e]	0.7	0.9
Na + - > Mg^{2+}	0.8[a]	0.7[c,d,e]	0.7	1.0
Na + - > Sr^{2+}	0.8[b]	0.7[c,d,e]	0.7	

[a] Based on correction method 2 and TBO data.
[b] Assumed to be the same as for Ca^{2+} and Mg^{2+}.
[c] Wersin et al. (2016).
[d] Kiczka et al. (2023).
[e] Pearson et al. (2011).
[f] Gaucher et al. (2009).
[g] Frederickx et al. (2018).

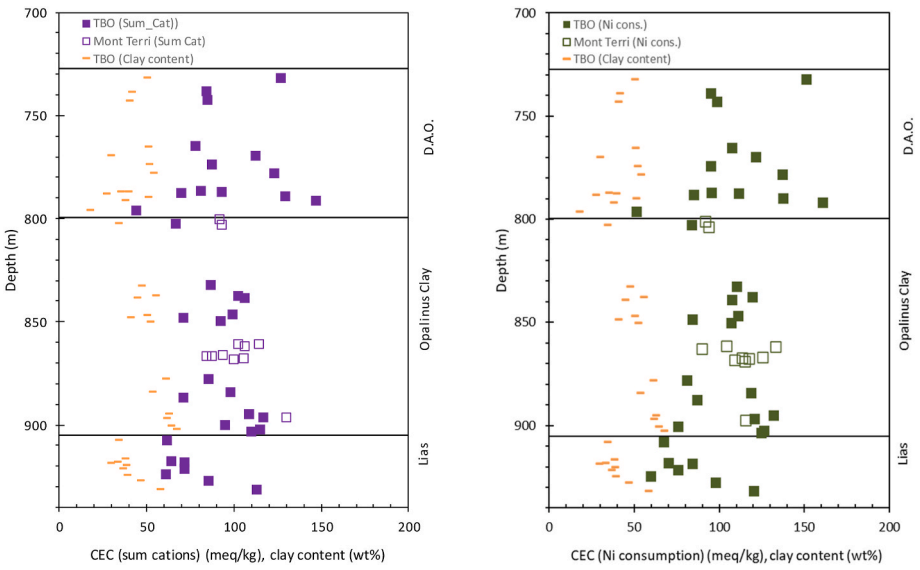

Fig. 2. Cation exchange capacities, shown as sum of cations (left) and Ni consumption (right) for TBO samples (filled) and Mont Terri samples (open). Clay content of TBO samples shown as orange symbols. Depth data are normalised to the profile of the STA2-1 borehole.

3. Results and discussion

3.1. Cation exchange capacities and cation occupancies

Cation exchange capacities, as determined from the (corrected) ΣCations (solid symbols) and Ni consumption (open symbols) are shown as a function of depth in Fig. 2. The CEC values of OPA samples scatter around 100 meq/kg without any clear trend. The upper confining unit (D.A.O.) exhibits a large range in CEC owing to the mineralogically more heterogeneous character of this unit (Section 2.1). The lower confining unit (Lias) also show some scatter in CEC values, but these suggest an increasing trend with depth.

CEC data obtained from the Σcations and from Ni consumption are consistent as indicated from the good agreement between these two datasets (Fig. 3 left). This supports the adequacy of the correction procedure for accounting for the extracted cations not related to the exchanger (dissolved in the porewater and resulting from mineral dissolution). However, a closer look reveals that the linear regression to the TBO data runs parallel, slightly above the 1:1 line. Thus, the CEC obtained from Ni consumption is systematically slightly higher compared to that obtained from Σcations (although in many cases within the analytical error). For Mont Terri samples, the trend is less clear owing to the larger scatter of the data. Higher values for Ni consumption relative to Σcations were also observed in previous studies (Bradbury and Baeyens 1998; Wersin et al., 2016; Hadi et al., 2019). Possible reasons for an apparent overconsumption of Ni were suggested to be (i) formation of polynuclear Ni surface complexes and/or Ni (co) precipitates and (ii) sorption of Ni^{2+} to amphoteric oxide-type surface sites. The Σcations and Ni consumption data show rather good agreement with the calculated CEC (CEC_{calc}, section 2.5) scattering around the 1:1 line, whereby Ni consumption tend to plot slightly below this line (Fig. 3 right). According to CEC_{calc} data, the largest share of the CEC is provided by illite making up 62% on average, followed by smectite (32%). The other two clay minerals chlorite and kaolinite thus contribute only to a minor extent to the CEC. In summary, both Ni consumption and Σcations data derived from the Ni-en extraction method are good proxies for the CEC, but the latter is slightly closer to the calculated CEC.

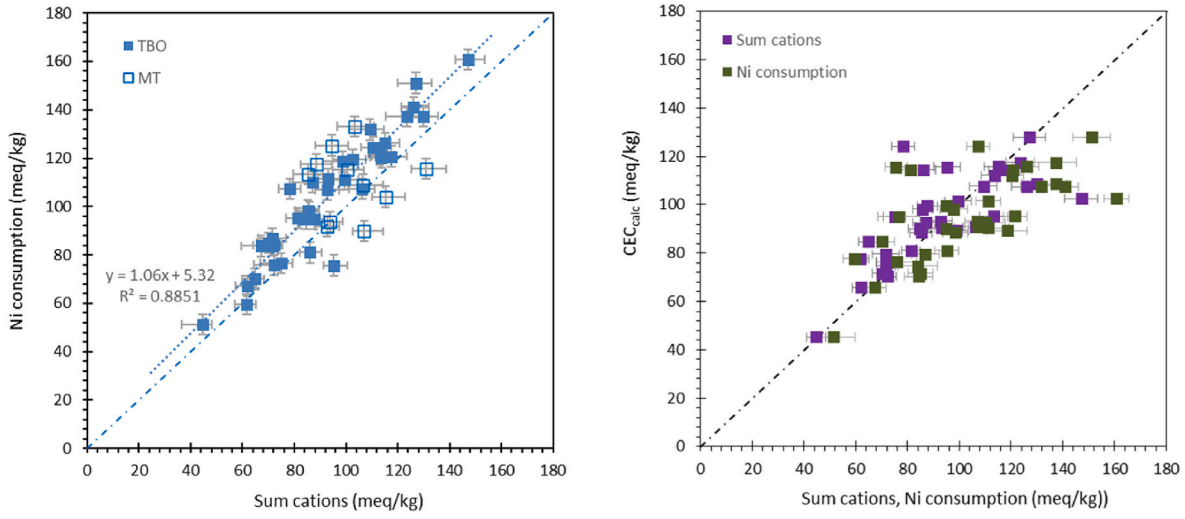

Fig. 3. Σcations vs. Ni consumption values (left) and Σcations, Ni consumption values vs. calculated CEC based on clay mineralogy (CEC_{calc}) (right). Dashed line: 1:1 relationship; dotted line left plot: linear regression. Note that for Mont Terri data no CEC_{calc} can be derived because of lack of clay mineral data.

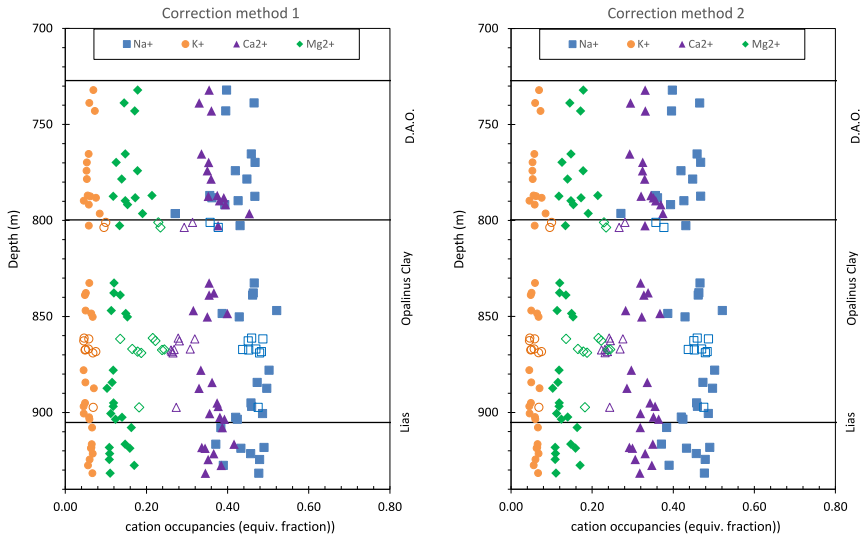

Fig. 4. Fractional occupancies of exchangeable cations as a function of depth based on correction method 1 (left) and correction method 2 (right). Closed symbols: TBO data; open symbols: Mont Terri data. Depth data are normalised to the profile of the STA2-1 borehole. D.A.O. = Dogger above Opalinus Clay.

The exchanger composition, given as fractional occupancies (equivalent fraction), as a function of depth is illustrated in Fig. 4. The solid symbols represent TBO data whereas the Mont Terri data are shown as open symbols. Fig. 4 (left) shows the exchanger composition based on correction method 1 in which both Cl and SO_4 are attributed to Na, leaving the other extracted cations Ca, Mg and K unchanged. The exchanger composition based on correction method 2, in which Cl is attributed to Na and SO_4 to Ca (leaving Mg and K unchanged) is shown in Fig. 4 right). Na and Ca are the main cations, followed by Mg and K irrespective of the correction method. Note that the Na occupancies are shifted to slightly lower values in method 1 relative to method 2 while the Ca occupancies are shifted to slightly lower values with the latter method.

With regard to the TBO data, the exchanger compositions are remarkably constant across the sampled 200 m thick sequence in spite of the variable CEC and clay content, in particular in the confining units above and below the OPA (Fig. 4).

Mont Terri data is similar as TBO data regarding monovalent cations Na and K but displays somewhat lower Ca and higher Mg occupancies. This point is further discussed in Section 3.3. Note that the Mont Terri data generally display a larger scatter in the Mg occupancies.

The distribution of cations in the porewaters (Fig. 5 left) shows a mirrored picture of the corresponding exchanger composition, with near-to-constant ratios across the geological sequence. Conversely, the ionic strength shows strong variations both laterally and vertically (Kiczka et al., 2023), as exemplified by the concentrations of chloride (Fig. 5 right), the main anion in all porewaters. This underlines the effectiveness of the clay exchanger to buffer the cationic distribution in the porewater (Wersin et al., 2020). The share of Na in the porewater is higher compared to the exchanger, indicating the larger selectivity of the other cations to the clay surface. This is quantitatively assessed in the following section. Mont Terri porewater data (open symbols) are in line with the ones from TBO (closed symbols) except for Mg, as discussed in section 3.3.

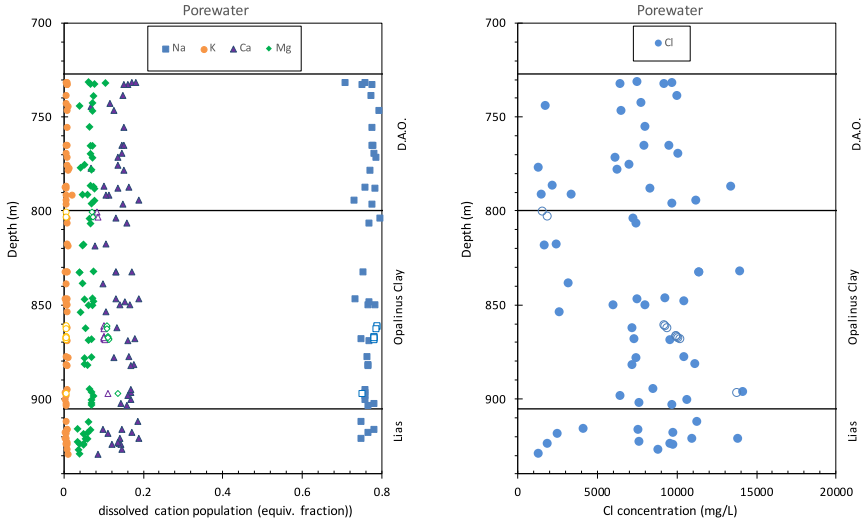

Fig. 5. Fractional occupancies of cations (left) and chloride concentrations (right) in the porewaters as a function of depth. Closed symbols: TBO data; open symbols: Mont Terri data. Depth data are normalised to the profile of the STA2-1 borehole. D.A.O. = Dogger above Opalinus Clay.

3.2. Selectivity coefficients

Knowing the exchanger and porewater composition, the latter being obtained from squeezing, advective displacement and borehole sampling, the selectivity coefficients (K_c) for the different cations with respect to Na^+ can be derived for each sample pair as detailed in Section 2.5.

The derived mean selectivity coefficients for K, Ca, and Mg for all samples as well as for the different units (D.A.O, OPA and Lias) from the TBO samples are listed in Table 1. Overall, no large differences in mean exchange parameters between the units are noted, but the data spread varies. Thus, the upper confining unit D.A.O shows the largest spread (cf. Standard deviation in Table 1), which is not surprising given the large variation in mineralogy, particularly regarding the clay content and clay mineralogy. The lower confining unit Lias, which is less heterogeneous and generally clay-rich, displays somewhat less spread but similar mean selectivity coefficients for K, Ca and Mg as the upper confining unit. The mean selectivity coefficients derived for OPA are similar but slightly lower than those of the confining units and the range is generally smaller.

Data from Mont Terri yields selectivity coefficients that are largely consistent with the ones from TBO. The Mont Terri samples show similar selectivity coefficients for K and Ca but a somewhat lower one for Mg as the TBO samples. Variations in exchanger composition are somewhat larger, especially regarding Mg data. This is perhaps related to slightly different experimental protocols used for the Ni-en extraction experiments for the Mont Terri samples which were acquired by different researchers over the last 20 years. The TBO data on the other hand was produced within a fairly short time frame (~3 years) using a refined protocol based on experiences gained before.

The propagated analytical uncertainty of the K_c values is about 10% for Na–K and about 12% for Na–Ca and Na–Mg selectivity coefficients, thus in any case lower than the standard deviation (1σ) on the mean values shown in Table 1.

The rather subtle differences between the derived selectivity coefficients in terms of variability and mean values for the confining units on the one hand and for OPA on the other are likely related to the more heterogeneous nature of the former units. Thus, clay content and clay mineralogy are more variable in the confining units compared to the rather homogeneous OPA. Fig. 6 shows the variation of the selectivity coefficient $K_c^{Na/K}$ as a function of clay content and illite/kaolinite ratio for the two confining units and the OPA. The scatter in selectivity coefficients is largest for the clay-poor lithologies of the confining units, especially towards higher $K_c^{Na/K}$ values (Fig. 6 left).

A notable difference between OPA and confining units lies in the relative share of kaolinite. The former formation displays lower and constant ratios of illite/kaolinite, thus a higher proportion of kaolinite and distinctly less variability compared to the confining units. Samples from these units with the large illite/kaolinite ratios show the largest variations of $K_c^{Na/K}$. Similar features are indicated for the selectivity coefficients of Na→ Ca and Na→ Mg (Figure A2, SM). In summary, the more heterogeneous character of the confining units compared to OPA, results in more variation of selectivity coefficients, especially for the clay-poor lithologies.

The selectivity coefficients show no to little dependence on chloride concentrations and, thus ionic strength, which vary by more than half an order of magnitude. As depicted in Figure A3 (SM) left, a rather large scatter and no clear trend is observed when considering the ensemble of the data (TBO and Mont Terri). A slight positive correlation ($r^2 = 0.095$) can be envisioned for $K_c^{Na/K}$, but $K_c^{Na/Ca}$ and $K_c^{Na/Mg}$ do not suggest any meaningful trend with ionic strength.

As outlined in Section 3.1, the CEC is predominantly made up by the illite and smectite components (smectite being "bound" in the mixed layer illite/smectite minerals). Exchange models for clayrocks and clayey soils based on illite and smectite contents have been proposed for example by Tournassat et al. (2009). Here we test the adequacy of a two-site model including illite and smectite to predict the exchanger composition of the samples from the OPA and confining units. Illite and smectite selectivity coefficients based on the Gaines-Thomas convention were taken from Bradbury and Baeyens (2003, 2009).

The cation occupancies calculated by the two-site model are compared with measured occupancies as illustrated in Fig. 7. For Na, Ca and Mg, the data scatter around the 1:1 line, displaying deviation <10% from this relationship for the OPA samples. For the confining units, the spread is somewhat larger, but most samples fall within 10% deviation too. This supports the adequacy of the two-site model for estimating the exchanger composition for the main cations, but on the other hand also supports the notion that the observed scatter in selectivity coefficients is to a significant part related to varying clay mineralogy. In the case of Na and Ca, the data corrected with method 1 (open symbols) tend to plot slightly above and below the 1:1 lines, respectively. Data corrected with method 2, on the other hand, do not indicate any systematic deviation from this line. This may suggest that method 2 yields Na and Ca occupancies closer to the "true" values, but it has to be considered that the underlying methodological and data uncertainties are considerable.

In the case of K, the two-site model generally underpredicts the occupancies, thus indicating a too low selectivity for this cation. The derived selectivity coefficients of the OPA samples are in fact higher than that reported for illite (Table 1). The same observation was made by Tournassat et al. (2009) upon modelling of COx data. According to these authors, the most likely reason for the higher selectivity of K in the clayrock compared to that of pure illite is related to differences in particle morphology and surface area.

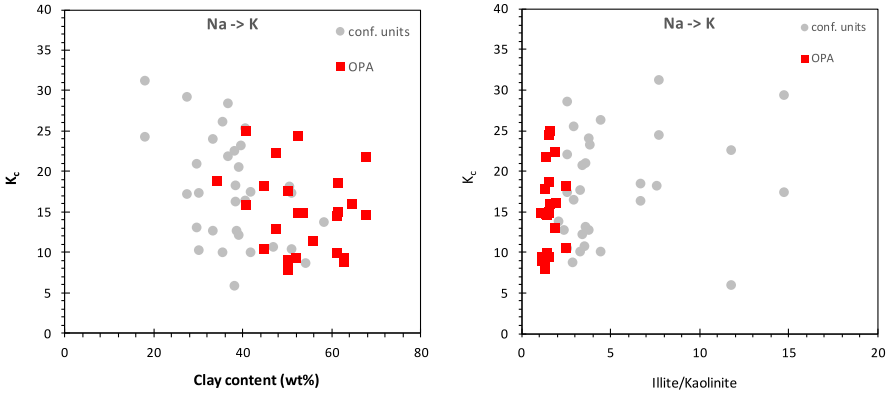

Fig. 6. Selectivity coefficients for Na–K as a function of clay content (left) and illite/kaolinite ratio (right).

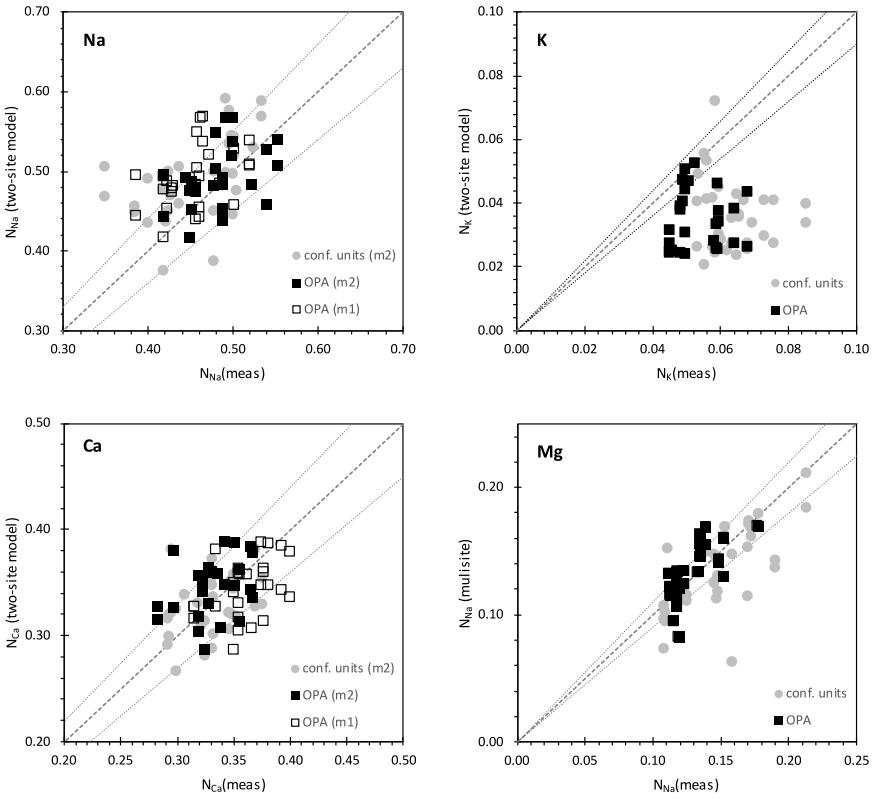

Fig. 7. Measured cation occupancies for samples from TBO (closed squares: method 2 correction, open squares: method 1 correction) vs. cation occupancies calculated from two-site (illite, smectite) model. Dashed line: 1:1 relation. Area between dotted lines: match between measured and calculated values within 10%.

3.3. Ca–Mg relationships

Calcite occurs in abundant amounts throughout the Opalinus Clay and its confining units. Moreover, dolomite is present in most lithologies, although its occurrence is patchier and less abundant (Mazurek et al., 2023). Assuming that the porewater is in equilibrium with these phases the activity ratio of Ca^{2+}/Mg^{2+} is fixed according to (Pearson et al., 2011):

$$\log(a_{Ca2+}/a_{Mg2+}) = 2\log K_{cc} - \log K_{do} \quad (5)$$

where is K_{cc} and K_{do} are the solubility constants of calcite and dolomite, respectively. Furthermore, according to eq. (2):

$$\log(N_{Ca}/N_{Mg} \times K_c^{Ca/Mg}) = 2\log K_{cc} - \log K_{do} \quad (6)$$

It has been shown by Kiczka et al. (2023) that the activity ratios of Ca^{2+}/Mg^{2+} of the porewaters extracted by squeezing and advective displacement are not constant but vary according to the formation temperature (Fig. 8 left). The same trend is seen for the ratio of Mg-to-Ca occupancies as illustrated in Fig. 8 right. The data points of TBO porewater samples lie clearly above the temperature dependent calcite-dolomite solubility line. This can be interpreted by the attainment of a new equilibrium with regard to calcite at room temperature, but not with regard to dolomite (Kiczka et al., 2023). The latter phase displays slow dissolution kinetics and, as mentioned above, a patchy

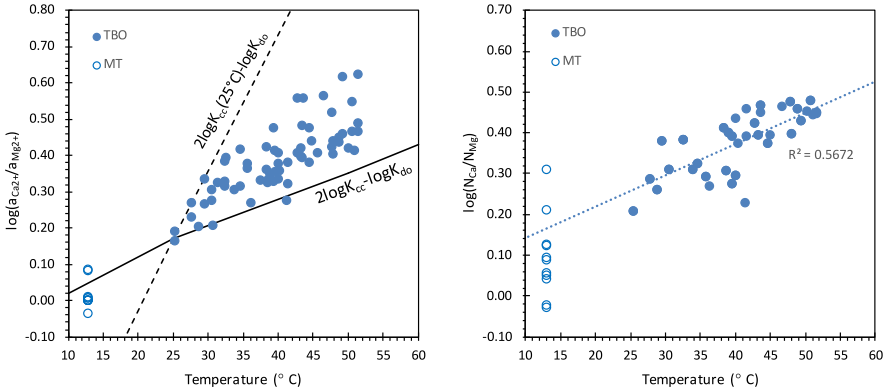

Fig. 8. Activity ratios of Ca^{2+}/Mg^{2+} in solution (left) and of N_{Ca}/N_{Mg} on exchanger (right) in log-units as a function of *in-situ* temperature. Solid line: calcite-dolomite equilibrium curve; dashed line: calcite-dolomite equilibrium curve assuming fixed calcite equilbirium at 25 °C (see text). Figure (left) modified from Kiczka et al. (2023). Thermodynamic data from THERMOCHIMIE database.

occurrence in the rock sequence. Assuming no dolomite dissolution at all but calcite re-equilibration upon cooling of the core samples would result in a steeper temperature dependence of log (a_{Ca2+}/a_{Mg2+}) (dashed line in Fig. 8 left). Most data points plot in between the two solubility lines. This suggests that some dolomite dissolution occurred as a result of lower temperature conditions under the assumption that calcite equilibrium was reached.

The Ca^{2+}/Mg^{2+} activity ratios of Mont Terri samples scatter around the calcite-dolomite solubility line (Fig. 8 left), suggesting close to equilibrium conditions of the porewaters with respect to these two phases at formation temperature (~13 °C). This is supported by the borehole water data at Mont Terri analysed by Wersin et al. (2022a) which is close to dolomite equilibrium. More scatter in the Mont Terri data is seen from the corresponding Ca/Mg ratios on the exchanger (Fig. 8 right) which is largely due to uncertainties in Mg occupancies, as also illustrated in Fig. 4 (open diamonds).

In contrast to a_{Ca2+}/a_{Mg2+} and N_{Ca}/N_{Mg} ratios, selectivity coefficients $K_c^{Ca/Mg}$ deduced for TBO data do not indicate any notable dependence with the *in-situ* temperature (Fig. 9 left). The data spread, however, becomes larger at higher *in-situ* temperature. Furthermore, selectivity coefficients seem quite independent of ionic strength, as represented by the chlorinity in Fig. 9 right and outlined already in Section 3.2. Note that for OPA samples, data scatter is smaller than for the confining units (compare red and grey points). The considerable spread in Mont Terri data can again be related to uncertainties regarding Mg occupancies.

3.4. Exchangeable Sr

Divalent Sr occurs only in minor amounts on the exchanger, its concentrations determined from Ni-en extraction are generally <1 meq/kg, well below those of Na, Ca, Mg and K. The analysis of exchangeable Sr is hampered by the dissolution of Sr bearing minerals, in particular celestite (Wersin et al., 2020; Kiczka et al., 2023). Celestite (containing variable amounts of Ba) was identified by scanning electron microscopy at Mont Terri (Pekala et al., 2019; Jenni et al., 2019), as well as in the Opalinus Clay and its confining units in deep boreholes in Northern Switzerland (Lerouge et al., 2014; Wersin et al., 2016; Jenni et al., 2019), but its distribution was found to be very inhomogeneous and its detection difficult.

Celestite equilibrium together with Sr^{2+} exchange is considered in modelling of porewater chemistry of Opalinus Clay for constraining sulphate and/or Sr concentrations (Pearson et al. 2003, 2011; Wersin et al., 2016; Kiczka et al., 2023). Celestite equilibrium is also corroborated by measured porewaters from squeezing, advective displacement and sampled boreholes (Wersin et al., 2020; Kiczka et al., 2023). Thus, knowing the exchangeable Sr fraction (together with those of the major cations) would be useful in this context, but, as mentioned above, the measurement thereof is affected by mineral dissolution during the extraction experiments. To estimate the difference between the measured and "true" exchange Sr, a simple modelling exercise based on porewater data has been carried out using PHREEQC. Thus, major cation and anion data from squeezing and advective displacement waters were considered, together with the CEC measured on the corresponding core samples. Updated exchange selectivity coefficients, which were derived as outlined in section 3.2., were applied. The selectivity coefficient of Sr ($K_c^{Na/Sr}$) was assumed to be the same as the ones of Ca and Mg (which are shown to be similar, see section 3.2). The corresponding value derived from data corrected by method 2 is 0.8 in log-units, which was applied for divalent cations Ca, Mg and Sr. For K, a selectivity coefficient of 1.2 (log-units) was considered (section 3.5).

The calculated Sr occupancies (open symbols) as a function of depth are illustrated in Fig. 10 left which also shows the measured data as obtained from Ni-en extraction (closed symbols). The latter values are systematically higher for the vast majority of data points, but the difference strongly varies. The largest mismatch is observed at the OPA/upper confining unit boundary where measured values are increased by about a factor of 4 relative to calculated values. It appears that Sr is enriched in this zone, presumably in the form of celestite. Assuming that this mineral is the only Sr-bearing phase reacting during Ni-en extraction, the dissolved amounts of $SrSO_4$ range from 10 to 40 mg/kg for most samples but may reach up to 100 mg/kg (Fig. 10 right). The contents of celestite is thus in any case very low (clearly below the XRD detection limit), but this rather soluble phase is important for constraining the porewater chemistry. It is in the same order of magnitude as the exchangeable Sr fraction.

3.5. Recommended selectivity coefficients for modelling

In summary, consistent exchange selectivity coefficients could be obtained from TBO and Mont Terri datasets. The derived values exhibit a narrow range considering the methodological uncertainties related to both the porewater and cation exchange parameters. It should be pointed out that the variation in exchanger composition is small, especially within the Opalinus Clay. On the other hand, ionic strength and chlorinity vary by half an order of magnitude, but this has only a minor effect on selectivity coefficients, which can thus be considered as largely independent of ionic strength. The same conclusion can be drawn for the formation temperature. The latter parameter seemingly affected Ca–Mg relationships, presumably because of slow dolomite reaction kinetics, but this, however, did not significantly affect selectivity coefficients. This suggests establishment of (new) cation exchange equilibria during the experimental runs at room temperature.

Derived selectivity coefficients indicate minor differences between the OPA and its upper and lower confining units (D.A.O. and Lias). The latter formations display larger mineralogical heterogeneity, also in

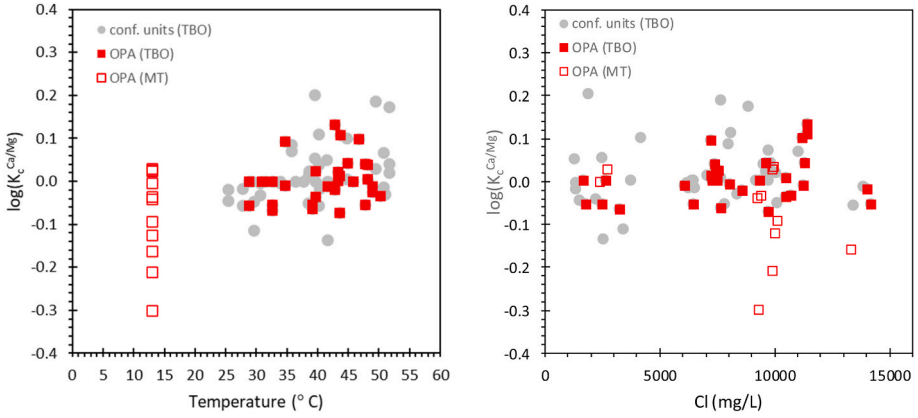

Fig. 9. Ca–Mg selectivity coefficients as a function of *in-situ* temperature (left) and of chloride concentration (right).

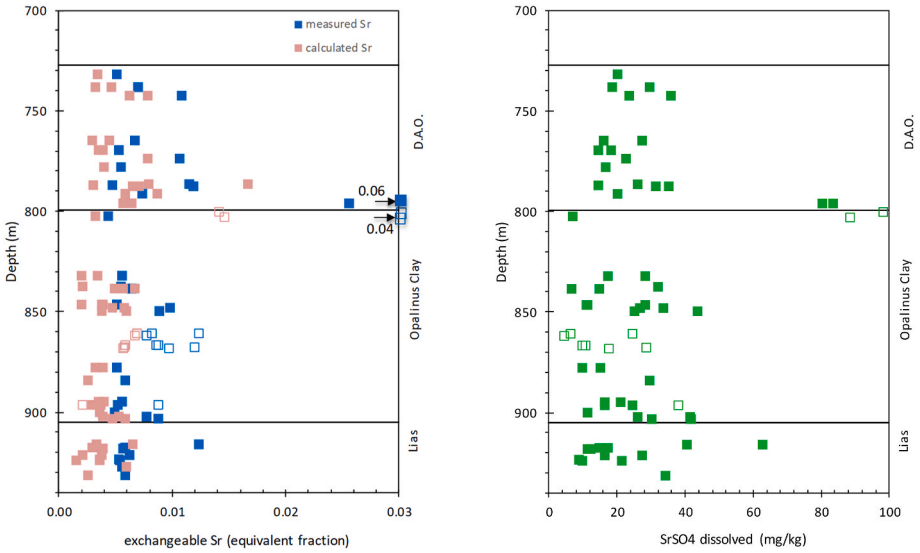

Fig. 10. Left: Measured (via Ni-en extraction) and calculated Sr occupancies as a function of depth. Right: Calculated amount of celestite that dissolved during Ni-en extraction based on the difference between measured and calculated Sr occupancies. Closed symbols: TBO data. Open symbols: Mont Terri data. Depth data are normalised to the profile of the STA2-1 borehole.

terms of clay mineralogy. The OPA, on the other hand, is characterised by a remarkably homogeneous clay mineralogy. A two-site exchange model including illite and smectite (the main carriers of the CEC) and published selectivity coefficients for these minerals were applied according to their shares in the respective OPA and confining unit samples. This showed that measured exchanger compositions could be fairly well matched for Na, Ca and Mg, but K occupancies were underpredicted. The simulated Na–Ca–Mg exchanger seems to be slightly more in line with the data obtained from correction method 2 relative to method 1, but the differences are small.

Table 2 summarises the selectivity coefficients obtained from the TBO data in log-units. The derived mean $\log K_c$ values together with uncertainty (1 σ) for all data as well as separately for OPA and confining units are shown. It underlines again the influence of the correction method for the contribution of dissolved salts on the derived selectivity coefficients, although this influence is not very large. There is a certain degree of arbitrariness and uncertainty related to the correction methods. The attribution of dissolved Cl to Na is reasonable in view of the systematic 1:1 relationship seen in aqueous extracts of these rocks (Pearson et al., 2003; Wersin et al., 2016; Aschwanden et al., 2024). The attribution of extracted SO_4, the second important anion, is less straightforward. A minor part of the porewater samples, namely from borehole BUL1-1 and BAC1-1 are close to saturation with regard to gypsum, whereas a major part shows undersaturation with regard to this mineral. Moreover, it has been shown that a large fraction of the sulphate released during aqueous and Ni-en extraction cannot be attributed to the porewater but to some unknown reaction occurring during the extraction process (Aschwanden et al., 2024). In view of the uncertainty inherent in the two correction methods, a third method was applied, in which the exchanger population was corrected according to the share of the corresponding cations in the porewater samples. Applying this method indicated a charge deficit of the cationic load relative to the anionic one (measured in the Ni-en extracts). Again, this can be related to the SO_4 in the Ni-en extracts which are higher than those in the porewaters. This "excess SO_4" was again distributed among the cations according to their share in the Ni-en extracts. The resulting selectivity coefficients of this method 3, which are also listed in Table 2, are similar to those derived from methods 1 and 2, but closer to the latter method. Thus, method 2 appears to yield fractional occupancies that seem to be closer to the *in-situ* values compared to method 1.

Table 3 summarises the proposed selectivity coefficients for OPA to be used for modelling. These are based on correction method 2 and on TBO data which indicates less scatter than Mont Terri data. It should be noted again that the derived selectivity coefficients are not independent of the applied correction method. However, the error introduced when for example using these selectivity coefficients for exchanger compositions derived with method 1 is small. In the same context, the use of the proposed values based on OPA data for confining units does not introduce large errors in the modelling.

As stated in the Introduction section, exchangeable cation data acquired by the Cs extraction method within the TBO programme (Marques Fernandes et al., 2024) were not used here because of the preferential mobilisation of K from illitic layers by that method. Scoping calculations carried out with OPA samples reported in Marques Fernandes et al., (2024) indicate that these data yield a higher $\log K_c^{Na/K}$ (≈1.5), but the corresponding selectivity coefficients for Na–Ca and Na–Mg are similar (≈0.9) to those obtained from Ni-en extraction.

The selectivity coefficients used in previous modelling exercises of OPA porewaters are also shown. As pointed out in the Introduction section, these are largely based on data generated for the COx Formation. The values are comparable to the ones established here, although values for Na–Ca and Na–Mg selectivity coefficients derived in this work are slightly higher. On the one hand this supports the validity of these previous modelling studies (differences in the modelling outcome would be minor). On the other hand, based on the present work modelling of cation exchange and porewater chemistry in OPA is put on more solid grounds.

The reported selectivity coefficients for the COx at the Bure site in France and the Boom Clay at the Mole site in Belgium, foreseen as host rocks for radioactive waste repositories, are also shown in Table 3. As noted above, the selectivity coefficients of the COx Formation (Gaucher et al., 2009) are similar as the ones derived for OPA. The exchanger composition of the COx Formation is dominated by divalent cations (Ca + Mg ≈ 75%) (Gaucher et al., 2006; Dohrmann et al., 2013), whereas that of OPA is exhibits similar shares of Na and Ca + Mg (Fig. 4). Regarding Boom Clay in Belgium, proposed selectivity coefficients (Frederickx et al., 2018) are somewhat higher, especially for Na–K. The high affinity of K in Boom Clay seems unexpected in view of the large amount of smectite in this clayrock, which is the main contributor to CEC (Frederickx et al., 2018). It might be related to the comparatively high amount of organic carbon in Boom Clay contributing to the CEC (Frederickx et al., 2018) and the potential chelating effect of organic

matter on K (Wang and Huang, 2001). Note that the porewaters of Boom Clay are of Na–HCO_3 type and rather dilute (ionic strength ~ 0.01 M) but display similar shares of the major exchangeable cations (Frederickx et al., 2018; Wang et al., 2023) compared to the studied OPA samples.

4. Conclusions

An extensive set of cation exchange data obtained from Ni-en extraction on the one hand and porewater chemistry data obtained from high-pressure squeezing and advective displacement on the other hand enabled the achievement of selectivity coefficients for major cations in the Opalinus Clay and its low permeability confining units. These data were acquired from drillcores of eight deep boreholes from a recent siting programme (TBO) for geological disposal of radioactive waste. The obtained values are consistent with those obtained in parallel from the Mont Terri rock laboratory although the scatter underlying exchangeable cation data is somewhat larger in the latter dataset. The exchanger compositions of the ensemble of samples are remarkably constant, both vertically and horizontally in spite of considerable variations of ionic strength.

The derived selectivity coefficients indicate no dependency on ionic strength or *in-situ* temperature of the samples, thus supporting their validity over a large range of salinity and *in-situ* temperature conditions. The latter parameter seemingly affected Ca–Mg relationships, but this did have a significant influence on the corresponding selectivity coefficients. The (rather subtle) differences in K_c values between OPA and confining units can be attributed to the differences in clay mineralogy. Based on data analysis, the most adequate correction method for considering the contribution of dissolved salts in the extract solutions when deriving the cation occupancies could be recommended. The validity of a simple two-site exchange model including illite and smectite for estimating exchangeable Na, Ca and Mg on the exchanger could be shown, but this model underpredicted the share of exchangeable K.

Exchangeable Sr could not be determined because of the dissolution of Sr-bearing minerals (mainly celestite). Based on mass balance considerations, the amounts of celestite in the rock are within the same order of magnitude as the exchangeable Sr fraction.

Recommended values for selectivity coefficients for OPA are similar to those used in previous modelling studies, confirming on the one hand their validity and providing a more solid basis for these studies on the other hand.

CRediT authorship contribution statement

Paul Wersin: Writing – original draft, Project administration, Methodology, Investigation, Data curation, Conceptualization. **Lukas Aschwanden:** Writing – review & editing. **Mirjam Kiczka:** Writing – review & editing, Data curation, Conceptualization.

Declaration of competing interest

The authors declare that they have no known competing financial interests or personal relationships that could have appeared to influence the work reported in this paper.

Data availability

Data will be made available on request.

Acknowledgements

This study was part of the large deep drilling campaign 2019–2022 in northern Switzerland led by the Swiss National Cooperative for the Disposal of Radioactive Waste (Nagra). For the present study, we would particularly like to thank Martin Mazurek, Andreas Jenni, Urs Mäder, Carmen Zwahlen, Thomas Gimmi (University of Bern), Maria Marques Fernandes, Bart Baeyens (PSI), Daniel Traber, Raphael Wüst (Nagra) for their contributions and fruitful discussions. We further express our thanks to Takahiro Oyama (CRIEPI, Japan) for support in porewater squeezing experiments. Financial support by Nagra is acknowledged. We appreciate the review comments which have helped to improve the manuscript.

Appendix A. Supplementary data

Supplementary data to this article can be found online at https://doi.org/10.1016/j.apgeochem.2024.106003.

References

Allard, B., Karlsson, M., Tullborg, E.-L., Larson, S.A., 1983. SKB Technical Report TR 83-64. Stockholm, Sweden.

Andra, 2005. Dossier 2005 argile. Référentiel de comportement des radionucléides et des toxiques chimiques d'un stockage dans le Callovo-Oxfordien jusqu'à l'homme. Site de Meuse/Haute Marne. Rapport Andra no. C.NT.AMES.03.046. Châtenay-Malabry, France.

Aschwanden, L., Camesi, L., Gimmi, T., Jenni, A., Kiczka, M., Mäder, U., Mazurek, M., Rufer, D., Waber, H.N., Wersin, P., Zwahlen, C., Traber, D., 2021. TBO Trüllikon-1-1: Data Report Dossier VIII. Rock properties, porewater characterisation and natural tracer profiles. Nagra Arbeitsbericht NAB 20-09,. Wettingen, Switzerland.

Aschwanden, L., Camesi, L., Gaucher, E., Gimmi, T., Jenni, A., Kiczka, M., Mäder, U., Mazurek, M., Rufer, D., Waber, H.N., Wersin, P., Zwahlen, C., Traber, D., 2023. TBO Stadel-3-1: Data Report Dossier VIII. Rock properties, porewater characterisation and natural tracer profiles. Nagra Arbeitsbericht NAB 22-01,. Wettingen, Switzerland.

Aschwanden, L., Wersin, P., Debure, M., Traber, D., 2024. Experimental study of water-extractable sulphate in the Opalinus Clay and implications for deriving porewater concentrations. Appl. Geochem. 160, 105837.

Baeyens, B., Bradbury, M.H. 1994. A physico-chemical characterisation and calculated in-situ porewater chemistries for a low permeability Palfris marl sample from Wellenberg. Nagra Technical Report NTB 94-22, Wettingen, Switzerland.

Baeyens, B., Marques Fernandes, M., 2022. Determination of the cation exchange capacities and exchangeable cations of deep drilling core samples from the siting regions Nördlich Lägern, Zürich Nordost and Jura Ost. Nagra Arbeitsbericht NAB 21–01,. Wettingen, Switzerland.

Beaucaire, C., Pearson, F.J., Gautschi, A., 2004. Chemical buffering capacity of clay rock. In Stability and Buffering Capacity of the Geosphere for Long-Term Isolation of Radioactive Waste, "Clay Club" Workshop Proceedings, pp. 147–154. Braunschweig, Germany, 9-11 December 2003, OECD 2004, NEA no. 5503.

Blanc, P., Legendre, O., Gaucher, E.C., 2007. Estimate of clay minerals amounts from XRD pattern modeling: the Arquant model. Phys. Chem. Earth, Parts A/B/C 32, 135–144.

Bossart, P., 2007. Overview of Key Experiments on Repository Characterization in the Mont Terri Rock Laboratory, vol. 284. Geol. Soc. London Spec. Publ., pp. 35–40, 284, 35-40.

Bossart, P., Bernier, F., Birkholzer, J., Bruggeman, C., Connolly, P., Dewonck, S., Fukaya, M., Herfort, M., Jensen, M., Matray, J.-M., 2017. Mont Terri rock laboratory, 20 years of research: introduction, site characteristics and overview of experiments. Swiss J. Geosci. 110, 3–22.

Bradbury, M.H., Baeyens, B., 1998. A physicochemical characterisation and geochemical modelling approach for determining porewater chemistries in argillaceous rocks. Geochim. Cosmochim. Acta 62, 783–795.

Bradbury, M.H., Baeyens, B., 2003. Porewater chemistry in compacted re-saturated MX-80 bentonite. J. Contam. Hydrol. 61, 329–338.

Bradbury, M.H., Baeyens, B., 2009. Sorption modeling on illite Part I: titration measurements and the sorption of Ni, Co, Eu and Sn. Geochim. Cosmochim. Acta 73, 990–1003.

Charlet, L., Alt-Epping, P., Wersin, P., Gilbert, B., 2017. Diffusive transport and reaction in clay rocks: a storage (nuclear waste, CO_2, H_2), energy (shale gas) and water quality issue. Adv. Wat. Resour. 106, 39–59.

Dohrmann, R., Olsson, S., Kaufhold, S., Sellin, P., 2013. Mineralogical investigations of the first package of the alternative buffer material test. II. Exchangeable cation population rearrangement. Clay Miner. 48, 215–233.

Frederickx, L., Honty, M., de Craen, M., Dohrmann, R., Elsen, J., 2018. Relating the cation exchange properties of the Boom Clay (Belgium) to mineralogy and porewater chemistry. Clays Clay Miner. 66, 449–465.

Gaucher, E.C., Blanc, P., Bardot, F., Braibant, G., Buschaert, S., Crouzet, C., Gautier, A., Girard, J.-P., Jacquot, E., Lassin, A., 2006. Modelling the porewater chemistry of the Callovian–Oxfordian formation at a regional scale. Compt. Rendus Geosci. 338, 917–930.

Gaucher, E.C., Tournassat, C., Pearson, F.J., Blanc, P., Crouzet, C., Lerouge, C., Altmann, S., 2009. A robust model for pore-water chemistry of clayrock. Geochim. Cosmochim. Acta 73, 6470–6487.

Gaucher, E.C., Aschwanden, L., Gimmi, T., Jenni, A., Kiczka, M., Mäder, U., Mazurek, M., Rufer, D., Waber, H.N., Wersin, P., Zwahlen, C., Traber, D., 2023. TBO Bachs-1-1: Data Report Dossier VIII. Rock properties, porewater characterisation and natural tracer profiles. Nagra Arbeitsbericht NAB 22-04,. Wettingen, Switzerland.

Giffaut, E., Grivé, M., Blanc, P., Vieillard, P., Colàs, E., Gailhanou, H., Gaboreau, S., Marty, N., Madé, B., Duro, L., 2014. Andra thermodynamic database for performance assessment: Thermochimie. Appl. Geochem. 49, 225–236.

Gimmi, T., Aschwanden, L., Camesi, L., Gaucher, E., Jenni, A., Kiczka, M., Mäder, U., Mazurek, M., Rufer, D., Waber, H.N., Wersin, P., Zwahlen, C., Traber, D., 2022. TBO Bözberg 2-1: Data Report Dossier VIII. Rock properties, porewater characterisation and natural tracer profiles. Nagra Arbeitsbericht NAB 21-22,. Wettingen, Switzerland.

Hadi, J., Wersin, P., Mazurek, M., Waber, H.N., Marques Fernandes, M., Baeyens, B., Honty, M., De Craen, M., Frederickx, L., Dohrmann, R., Fernandez, A.M., 2019. Intercomparison of CEC method within the GD project. Mont Terri Technical Report 2017-06.

Jenni, A., Lanari, P., Aschwanden, L., de Haller, A., Wersin, P., 2019. Spectroscopic Investigation of Sulphate-Controlling Phases in OPA, vols. 19–23. Nagra Arbeitsbericht, Wettingen, Switzerland.

Karnland, O., Olsson, S., Nilsson, U., 2006. Mineralogy and sealing properties of various bentonites and smectite-rich clay materials. SKB Technical Report TR-06-30, Stockholm, Sweden.

Kiczka, M., Wersin, P., Mazurek, M., Zwahlen, C., Jenni, A., Mäder, U., Traber, D., 2023. Porewater composition in clay rocks explored by advective displacement and squeezing experiments. Appl. Geochem. 159, 15838.

Koroleva, M., Lerouge, C., Mäder, U., Claret, F., Gaucher, E., 2011. Biogeochemical processes in a clay formation in situ experiment: Part B – results from overcoring and evidence of strong buffering by the rock formation. Appl. Geochem. 26, 954–966.

Lehmann, L., 2021. Herkunft von Sulfat im Porenwasser des Opalinustons. Bachelor's thesis (unpubl.). Institute of Geological Sciences, University of Bern, Switzerland.

Lerouge, C., Grangeon, S., Claret, F., Gaucher, E.C., Blanc, P., Guerrot, C., Flehoc, C., Wille, G., Mazurek, M., 2014. Mineralogical and isotopic record of diagenesis from the Opalinus Clay formation at Benken, Switzerland: implications for the modeling of pore-water chemistry in a clay formation. Clays Clay Miner. 62, 286–312.

Mäder, U., Aschwanden, L., Camesi, L., Gimmi, T., Jenni, A., Kiczka, M., Mazurek, M., Rufer, D., Waber, H.N., Wersin, P., Zwahlen, C., Traber, D., 2021. TBO Marthalen-1-1: Data Report Dossier VIII. Rock properties, porewater characterisation and natural tracer profiles. Nagra Arbeitsbericht NAB 21-20.

Marques Fernandes, F.M., Wersin, P., Mazurek, M., Wüst, R.A.J., Baeyens, B., 2024. Cation-exchange properties of the Mesozoic sedimentary sequence of northern Switzerland and modelling of the Opalinus Clay porewater. Appl. Geochem. 162, 105852.

Mazurek, M., Oyama, T., Wersin, P., Alt-Epping, P., 2015. Pore-water squeezing from indurated shales. Chem. Geol. 400, 106–121.

Mazurek, M., Aschwanden, L., Camesi, L., Gimmi, T., Jenni, A., Kiczka, M., Rufer, D., Waber, H.N., Wanner, P., Wersin, P., Traber, D., 2021. TBO Bülach-1-1: data Report Dossier VIII. Rock properties, porewater characterisation and natural tracer profiles. Nagra Arbeitsbericht NAB 20-08,. Wettingen, Switzerland.

Mazurek, M., Gimmi, T., Zwahlen, C., Aschwanden, L., Gaucher, E.C., Kiczka, M., Rufer, D., Wersin, P., Marques Fernandes, M., Glaus, M., Van Loon, L., Traber, D., Schnellmann, M., Vietor, T., 2023. Swiss deep drilling campaign 2019–2022: geological overview and rock properties with focus on porosity and pore-space architecture. Appl. Geochem. 159, 105839.

McBride, M., 1994. Environmental Chemistry of Soils. Oxford Press, New York.

Nagra, 2002. Projekt Opalinuston: Synthese der geowissenschaftlichen Untersuchungsergebnisse, Nagra Technical Report NTB 02-03. Wettingen, Switzerland.

Nagra, 2014. Sicherheitstechnischer Bericht zu SGT Etappe 2. Sicherheitstechnischer Vergleich und Vorschlag der in Etappe 3 weiter zu untersuchenden geologischen Standortgebiete. Nagra Technical Report NTB 14-01. Wettingen, Switzerland.

Ondraf/Niras, 2001. SAFIR 2 Safety Assessment and Feasibility Interim Report 2. ONDRAF/NIRAS Report Nirond 2001-06E, Brussels, Belgium.

Parkhurst, D.L., Appelo, C.A.J., 2013. Description of Input and Examples for PHREEQC Version 3: a Computer Program for Speciation, Batch-Reaction, One-Dimensional Transport, and Inverse Geochemical Calculations. US Geological Survey. No. 6-A43.

Pearson, F.J., Arcos, D., Bath, A., Boisson, J.Y., Fernández, A.M., Gäbler, H.-E., Gaucher, E., Gautschi, A., Griffault, L., Hernán, P., Waber, H.N., 2003. Geochemistry of water in the Opalinus clay formation at the Mont Terri rock laboratory. Federal Office for Water and Geology,. Bern, Series No. 5.

Pearson, F.J., Tournassat, C., Gaucher, E.C., 2011. Biogeochemical processes in a clay formation in situ experiment: Part E – equilibrium controls on chemistry of pore water from the Opalinus Clay, Mont Terri underground research laboratory, Switzerland. Appl. Geochem. 26, 990–1008.

Pekala, M., Wersin, P., Rufer, D., Curti, E., 2019. GD experiment: geochemical Data experiment. Mineralogy of carbonate and sulphate minerals in the Opalinus Clay and adjacent formations. Mont Terri Technical Report 2018-03.

Rodriguez, J., Colàs, E., Gailhanou, H., Duro, L., Fuller, A.J., Harvey, L., 2022. Track-changes and Track-Error Document: from Version 10d to Version 11. ThermoChimie Technical Report TCIII-2022-06e-Vs1.

Rufer, D., Stockhecke, M., 2021. Field Manual: Drill Core Sampling for Analytical Purposes. Nagra Arbeitsbericht NAB 19-13 Rev.1. Nagra, Wettingen, Switzerland.

RWI, 2020. SGT-E3 Deep Drilling Campaign (TBO): Experiment Procedures and Analytical Methods at RWI. University of Bern, Wettingen, Switzerland. April 2020). Nagra Arbeitsbericht NAB 20-13, Version 1.0.

Thellier, C., Sposito, G., 1989. Influence of electrolyte concentration on quaternary cation exchange by Silver Hill illite. Soil Sci. Soc. Am. J. 53, 705–711.

Tournassat, C., Gailhanou, H., Crouzet, C., Braibant, G., Gautier, A., Lassin, A., Blanc, P., Gaucher, E.C., 2007. Two cation exchange models for direct and inverse modelling of solution major cation composition in equilibrium with illite surfaces. Geochim. Cosmochim. Acta 71, 1098–1114.

Tournassat, C., Gailhanou, H., Crouzet, C., Braibant, G., Gautier, A., Gaucher, E.C., 2009. Cation exchange selectivity coefficient values on smectite and mixed-layer illite/smectite minerals. Soil Sci. Soc. Am. J. 73, 928–942.

Tournassat, C., Vinsot, A., Gaucher, E.C., Altmann, S., 2015. Chemical conditions in clay-rocks. In: Tournassat, C., et al. (Eds.), Natural and Engineered Clay Barriers, Developments in Clay Science 6. Elsevier, pp. 71–100 (Chapter 3).

Waber, H.N., Gaucher, E.C., Fernandez, A.M., Bath, A., 2003. Aqueous leachates and cation exchange properties of Mont Terri claystones. In: Pearson et al. (2003), Annex 1. Federal Office for Water and Geology,. Bern, Series No. 5.

Wang, F., Huang, P., 2001. Effects of organic matter on the rate of potassium adsorption by soils. Can. J. Soil Sci. 81, 325–330.

Wang, L., Honty, M., De Craen, M., Frederickx, L., 2023. Boom clay pore-water geochemistry at the Mol site: chemical equilibrium constraints on the concentrations of major elements. Appl. Geochem. 148, 105541.

Wersin, P., Mazurek, M., Mäder, U.K., Gimmi, T., Rufer, D., Lerouge, C., Traber, D., 2016. Constraining porewater chemistry in a 250 m thick argillaceous rock sequence. Chem. Geol. 434, 43–61.

Wersin, P., Pekala, M., Mazurek, M., Gimmi, T., Mäder, U.K., Jenni, A., Rufer, D., Aschwanden, L., 2020. Porewater Chemistry of Opalinus Clay: Methods, Modelling & Buffering Capacity. Nagra Technical Report, Wettingen, Switzerland. NTB 18-01.

Wersin, P., Mazurek, M., Gimmi, T., 2022a. Porewater chemistry of Opalinus clay revisited: Findings from 25 years of data collection at the Mont Terri rock laboratory. Appl. Geochem. 138, 105234.

Wersin, P., Aschwanden, L., Camesi, L., Gaucher, E.C., Gimmi, T., Jenni, A., Kiczka, M., Mäder, U., Mazurek, M., Rufer, D., Waber, H.N., Zwahlen, C., Traber, D., 2022b. TBO Bözberg 1-1: Data Report Dossier VIII. Rock properties, porewater characterisation and natural tracer profiles. Nagra Arbeitsbericht NAB 21–21. Wettingen, Switzerland.

Zwahlen, C., Aschwanden, L., Camesi, L., Gaucher, E., Gimmi, T., Jenni, A., Kiczka, M., Mäder, U., Mazurek, M., Roos, D., Rufer, D., Waber, H.N., Wersin, P., Traber, D., 2022. TBO Stadel-2-1: Data Report Dossier VIII. Rock properties, porewater characterisation and natural tracer profiles. Nagra Arbeitsbericht NAB 22-02,. Wettingen, Switzerland.